Evaluation the cytotoxic effect of Fe$_3$O$_4$@Glu-Gingerol on lung adenocarcinoma cell line (A549) with biological mechanisms

Tabarek Abdulrazaq Alkinani [a,1], Fahimeh Abedini Bajgiran [b,1],
Mohammad Rezaei [c,1], Ali Motamedi Maivan [b,1], Fatemeh Jafari Golrokh [b,1],
Mona Bejarbaneh [b,1], Sara Rezaei Mojdehi [b,1], Sahar Gorji [b,1], Reza Ghasemian [d,1],
Mohammad Dashtban Jalil Pustin Sarai [b,1], Fatemeh Akbari [e,1],
Somayeh Dehghan [f,1], Fatemeh Mirzaee [b,1], Noor Hussein Abdulrahman [a,1],
Ali Salehzadeh [b,*]

[a] College of Pharmacy, Al-zahraa University for Women, Iraq
[b] Department of Biology, Rasht Branch, Islamic Azad University, Rasht, Iran
[c] Iranian Research Organization for Science and Technology, Tehran, Iran
[d] Department of Medical Sciences, Faculty of Medicine, Tehran Medical Sciences, Islamic Azad University, Tehran, Iran
[e] Department of Biology, Faculty of Basic Sciences, Shahrekord Branch, Islamic Azad University, Shahrekord, Iran
[f] Department of Biology, Central Tehran Branch, Islamic Azad University, Tehran, Iran

ARTICLE INFO

ABSTRACT

The use of nanotechnology products with supermagnetic properties for targeted delivery of drugs has gained attention recently. Due to the anticancer features of Gingerol, the major phenolic compound from Ginger, this study aims to prepare Fe$_3$O$_4$@Glucose-Gingerol nanoparticles (NPs) and investigate their anticancer potential in a lung adenocarcinoma cell line. The physical and chemical features of the nanoparticles were investigated by FT-IR, XRD, zeta potential, DLS, EDS mapping, VSM, and electron microscope imaging. Cytotoxic effects of the nanoparticles for the A549 (lung adenocarcinoma) and MRC-5 (normal) cell lines was investigated by MTT assay. Furthermore, the effects of Fe$_3$O$_4$@Glucose-Gingerol nanoparticles on the expression of the *CASP8*, *BAX*, and *BCL2* genes and the activity of Caspase 3 were characterized. The flow cytometry assay (annexin V/PI) was employed to find out the percentage of apoptotic cells. The Fe$_3$O$_4$@Glu-Gingerol NPs were spherical (42–67 nm), without elemental impurity, and with surface charge, DLS size, and magnetic saturation of -47.7 mV, 154 nm, and 35 emu/g, respectively. Fe$_3$O$_4$@Glu-Gingerol NPs showed a remarkable greater toxicity in the A549 cells than normal cell line with the 50 % inhibition concentration (IC$_{50}$) of 190 and 554 μg/mL, respectively. Treatment of lung adenocarcinoma cells with the Fe$_3$O$_4$@Glu-Gingerol NPs led to an increase in cell apoptosis from 4.6 to 39.48 %. Also, the *CASP8* and *BAX* genes were upregulated by 2.49 and 2.8 folds, respectively, while a downregulation by 0.75 folds was noticed for the *BCL2*. Moreover, apoptotic features were observed in Fe$_3$O$_4$@Glu-Gingerol NPs treated cells by Hoechst staining, and activation of Caspase 3 by 2.8 folds. This study revealed that the Fe$_3$O$_4$@Glu-Gingerol NPs have antiproliferative effects on the lung adenocarcinoma cell line by activation of intrinsic and extrinsic apoptosis that is a promising feature in cancer treatment.

1. Introduction

Lung cancer is the second most frequent cancer which causes more than 2,200,000 annual new cases in the human population. This disease is the most fatal cancer in both genders and is associated with one-fifth of cancer-associated death. According to the statistics, the disease is responsible for almost annual 1,800,000 deaths [1]. The large mortality of lung cancer indicates the poor diagnosis approaches and the absence of effective medicinal compounds. Therefore, many studies aim to find novel anticancer agents to be used against lung cancer.

Many nanotechnology products have been explored in cancer diagnosis, prevention, and treatment. Owing to the large surface area and small size, these particles could distribute to the host body and reach their target site. However, the low efficacy and specificity of such compounds result in undesirable effects which could limit their applications in disease diagnosis and treatment [2]. Therefore, recent studies aim to provide modified NPs to improve their biocompatibility, therapeutic efficacy, and reduce their unwanted features.

Iron oxide (Fe_3O_4) NPs have received considerable attention in biomedical fields. These compounds are biocompatible, biodegradable, and potentially non-toxic to the human [3,4]. In addition, owing to their supermagnetic property, these NPs could be magnetized when an external magnetic field is applied [3]. This feature enables Fe_3O_4 NPs to be used for site directed delivery which significantly increases the efficacy and reduces undesirable side-effect of the therapeutic molecules. Therefore, Fe_3O_4 nanoparticles can be a platform for the design and development of multi-agent anticancer drugs. Functionalization of Fe_3O_4 NPs with small molecules or polymers can enhance the biodistribution of the particles and lead to longer circulation time and more efficient uptake. Newly, carbohydrates, as biomimetic functional molecules, have gained interests to be used for surface functionalization nanoparticles. Functionalization with glucose may facilitate nanoparticle internalization via specific cellular receptors. By modulating oxidative stress and cellular uptake, functionalization of Fe_3O_4 with Glucose can improve their biocompatibility and anticancer potential [5,6].

Phytochemical compounds that are naturally found in medicinal plants have gained interests to prevent and treat diseases. Gingerols are the bioactive compounds found in the root of Ginger that show antioxidant, anti-inflammation, and antitumor activities [7, 8].

According to the literature, multiple mechanisms are involved in the anticancer effect of gingerol, including increasing the expression of some proapoptotic genes such as NAG-1 and inhibiting cell cycle progression by attenuation of cyclin D1 [9]. Furthermore, down-regulation of the expression of Akt and up-regulation of the expression of *BAX/BCL-2* have been associated with the inhibitory effect of gingerol on cancer cells [10]. Moreover, the caspase-dependent apoptogenic properties of gingerol and inhibition of cell proliferation through inhibiting the MAPK/AP-1 signaling have been described in the literature [11].

Due to the biomedical properties of gingerol, in this study, gingerol was conjugated to Fe_3O_4 NPs via glucose functionalization, and the anticancer effect of the Fe_3O_4@Glu-Gingerol nanoparticles on a lung adenocarcinoma cell line and their effect on the expression of *CASP8*, *BAX*, and *Bcl2* cells were studied.

2. materials and methods

2.1. Synthesis of Fe₃O₄ nanoparticles

At first, 5.75 g FeCl₃.6H2O and 3.17 g FeCl₂.4H2O were suspended in distilled water and maintained at 80 °C for 60 min and then, an NH₃ solution was added. After maintaining the mixture at 80 °C for 180 min, the pellet was collected, washed with ethanol and distilled water, and dried [12].

2.2. Preparation of Fe₃O₄@Glu-Gingerol

At first, a suspension containing Fe_3O_4 (1.6 %) and 0.5 g D-glucose (0.8 %) was prepared in distilled water, sonicated for 30 min, and then, autoclaved at 180 °C for 3 h. After centrifugation at 6000 rpm, the pellet was washed three times and finally, dried at 60 °C.

$$5.75 \text{ g FeCl}_3.6\text{H2O} + 3.17 \text{ g FeCl}_2.4\text{H2O} + 300 \text{ mL dH}_2\text{O} \longrightarrow Fe_3O_4 \text{ NPs}$$

$$1\text{g Fe}_3O_4 \text{ NPs} + 0.5 \text{ g D-Glucose(C}_6\text{H}_{12}\text{O}_6) \longrightarrow Fe_3O_4@\text{Glu NPs}$$

$$1 \text{ g Fe}_3O_4@\text{Glu NPs} + 0.1 \text{ g Gingerol (C}_{17}\text{H}_{26}\text{O}_4) \longrightarrow Fe_3O_4@\text{Glu- Gingerol NPs}$$

To prepare conjugated NPs, 1 g of Fe_3O_4@Glu and 100 mg of gingerol were dispersed in distilled water and shaked for 24h. After centrifugation at 6000 rpm, the Fe_3O_4@Glu-Gingerol NPs were harvested, dried, and lyophilized (steps 1–2 and 2-2 are shown in the following formula).

2.3. Physical and chemical characteristics of the synthesized NPs

Characterization of the nanoparticles was performed by FT-IR, XRD, TEM, SEM, EDS-mapping, DLS, and Zeta potential analyses. FT-IR assay was performed by a PerkinElmer FT-IR spectrophotometer (USA) in a range of 400–4000 cm^{-1}. The crystalline structure of

NPs was evaluated by XRD analysis at k = 1.79 Å (Philips, PW1730, Netherland). Electron microscopy was performed by TESCAN Mira3 SEM (Czech Republic) and Zeiss EM-900 TEM (Germany) microscopes. The elemental composition was assayed by EDS-mapping (TESCAN Mira3, Czech Republic) and magnetization level of Fe_3O_4@Glu-Gingerol was studied by a magnetometer (Meghnatis Dag-high Kavir Co., Kashan, Iran). Finally, the DLS size and zeta-potential of Fe_3O_4@Glu-Gingerol were determined by a HORIBA Scientific SZ-100 Zeta sizer (Japan).

2.4. Cytotoxic effect of Fe_3O_4@Glu-Gingerol

To determine the cytotoxicity of Fe_3O_4@Glu-Gingerol and Fe_3O_4 NPs, lung adenocarcinoma cell line (A549) and human normal cell line (MRC-5) were grown in DMEM (Dulbecco's modified Eagle medium) medium. Also, the cytotoxic activity of gingerol on the A549 cell line was determined. After cell propagation in 96-well plates (1×10^4), different concentrations of Fe_3O_4@Glu-Gingerol, gingerol and Fe_3O_4 NPs (62.5–1000 μg/mL) were added to the wells and incubated at 37 °C for 24 h, cell viability level was evaluated using the 2-(4,5-dimethythiazol-2-yl) −2,5-diphenyltetrazolium bromide (MTT) assay. In brief, 0.2 mL of MTT solution was added to the wells and incubated for 4h. Then, the wells were emptied and 0.1 mL of dimethyl sulfoxide (DMSO) was added. After shaking the plate for 30 min at room temperature, the OD_{570} of the wells was recorded (Bio-Rad plate reader, Hercules, CA, USA) [13]. The percentage of inhibition was calculated by the following formula [14]. The inhibitory potential of the nanoparticles was calculated as follows:

$$Inhibition~(\%) = \frac{Abs~of~control - Abs~of~Test}{Abs~of~control} \times 100$$

2.5. Flow cytometry assay

To evaluate the frequency of cell apoptotic in Fe_3O_4@Glu-Gingeroil and control cells a flow cytometry analysis was conducted. Monolayers of cancer cells (1×10^6) were prepared and treated with the NPs. Then, the cells were harvested, washed with phosphate buffered saline, and subjected to the propidium iodide and Annexin V (Roche, Germany) staining. Finally, apoptosis level in the control and nanoparticle-treated cells was evaluated by a flow cytometry device (BIO-RAD, USA).

2.6. Expression of CASP8, BAX, and BCL2 genes

Real-time PCR assay was used to find out the effect of Fe_3O_4@Glu-Gingerol and Fe_3O_4 NPs on the expression of the pro- and anti-apoptotic genes, including *CASP8*, *BAX*, and *BCL2*. At first, lung adenocarcinoma cells (5×10^5) were treated with the NPs (at IC_{50}) for 24 h and then, their RNA content was extracted (TriZol, Sigma-Aldrich, USA). After characterization of the quality of RNA samples using Nanodrop spectrophotometry (NanoDrop™ 2000/2000c, Thermo Scientific, USA), cDNA molecules were synthesized using a Yekta Tajhiz cDNA synthesis Kit (Iran). Finally, qPCR assay was performed using the primers presented in Table 1 to find out the expression level of the *CASP8*, *BAX*, and *BCL2* genes under treatment of Fe_3O_4@Glu-Gingerol and Fe_3O_4 NPs. The *GAPDH* gene was used as a control gene and the gene expression level was calculated by the $2^{-\Delta\Delta Ct}$ method [15].

2.7. Caspase 3 activity assay

Caspase 3 activity under treatment of Fe_3O_4@Glu-Gingerol and Fe_3O_4 NPs on cancer and control cells (1×10^6) was assayed [13]. At first, the cells were treated with the nanoparticles for 24h, and then, were washed with PBS, and lysed. Finally, the supernatant was treated with DEVD-pNA (Sigma-Aldrich, CASP3C) and optical density at 405 nm was measured.

2.8. Hoechst staining

Nuclear morphological alterations caused by Fe_3O_4@Glu-Gingerol were investigated by Hoechst nuclear staining. After incubating cancer cells with the nanoparticles, the cells were washed, stained with the Hoechst 33,258, and examined under a fluorescent microscope [13].

Table 1
Sequence of the primers used in this work.

Primer	Sequence (5'-3')	Product size (bp)	Reference
Bax-forward	TTGCTTCAGGGGTTTCATCCA	113	[16]
Bax-reverse	AGACACTCGCTCAGCTTCTTG		
CASP8-forward	GACTGGATTTGCTGATTACCTACCTAA	143	[17]
CASP8-reverse	CCTCAATTCTGATCTGCTCACTTCT		
Bcl2-forward	TGGCCAGGGTCAGAGTTAAA	147	[16]
Bcl2-reverse	TGGCCTCTCTTGCGGAGTA		
GAPDH-forward	CCCACTCCTCCACCTTTGAC	75	[17]
GAPDH-reverse	CATACCAGGAAATGAGCTTGACAA		

2.9. Statistical analyses

The SPSS. 16.0 software and one-way ANOVA analysis were used to evaluate the statistical difference between the NPs treated and control cells. The assays were performed in three replicates and the p-value<0.05 was considered significant.

3. results

3.1. Physiochemical characteristics of nanoparticles

Investigation of functional groups of Fe_3O_4@Glu-Gingerol revealed absorption peaks at 420, 580, and 624 nm that are associated with the Fe–O bonds and related to the Fe^{+2} and Fe^{+3} atoms at their tetragonal phase and Fe^{+3} atom at its octagonal phase that present the formation of Fe_3O_4 structure. Also, the peaks at 598, 815, 902, and 1034 nm are related to the C–C, C–H, =CH, and C–O of the gingerol molecule. In addition, the peak at 1401 nm is associated with the C–C bond of the benzene ring. Furthermore, the peaks at 1641, 2904, and 3406 nm are related to the C=C and OH bonds. The FT-IR spectrogram reveals the proper synthesis of Fe_3O_4@Glu-Gingerol (Fig. 1).

Based on the XRD pattern, the diffraction peaks at 30, 35, 43, 57, and 63° correspond to the Fe_3O_4 particles (JCPDS card no: 03–0863). Also, the peaks at 10–20° could be associated with the amorphous structures of gingerol. According to Scherrer formula, the average size of crystals was 7.07 nm. Fig. 2 presents the XRD analysis of Fe_3O_4@Glu-Gingerol NPs.

According to the SEM (Fig. 3a and d) and TEM (Fig. 3c and b) images the Fe_3O_4@Glu-Gingerol particles were spherical and were in a size range of 42–67 nm. The surface charge and DLS size of Fe_3O_4@Glu-Gingerol were −47.7 mv and 154 nm, respectively (Fig. 4a and c). Meanwhile, the surface charge and DLS size of Fe_3O_4 NPs were measured −11.9 mv and 96 nm, respectively (Fig. 4b and d). The more negative surface charge of Fe_3O_4@Glu-Gingerol provides sufficient repulsive force to reduce particle aggregation. According to the EDS and mapping results, the NPs contained Fe, C, and O molecules (Fig. 5a and b). The VSM analysis revealed the magnetic feature of the synthesized NPs. The maximum magnetization saturation of Fe_3O_4@Glu-Gingerol NPs was measured 35 Emu/g, which was displayed in Fig. 6.

3.2. Cytotoxicity of Fe_3O_4@Glu-Gingerol NPs

According to the results, the nanoparticles had significant toxic effects on cancer cells which reduced the viability of the cells by 15–85 %, depending on the exposure dose. Calculating the IC_{50} of Fe_3O_4@Glu-Gingerol NPs for lung cancer and normal human cells showed that the nanoparticles were significantly more toxic for cancer cells ($IC_{50} = 190$) than normal cells ($IC_{50} = 554$ µg/mL) (Fig. 7a, b). Also, the IC_{50} of Gingerol and Fe_3O_4 NPs for A549 cell line was 248 µg/mL and 531 µg/mL, respectively (Fig. 7c,d).

3.3. Flow cytometry analysis

The results revealed that the nanoparticles considerably increase cell apoptosis among treated cells. The percentage of the early and late apoptosis in nanoparticle-treated cells was 4.33 and 35.15 %, respectively. In contrast, the early and late apoptosis in control cells were 0.28 and 0.18 %, respectively. The results were presented in Fig. 8a and b.
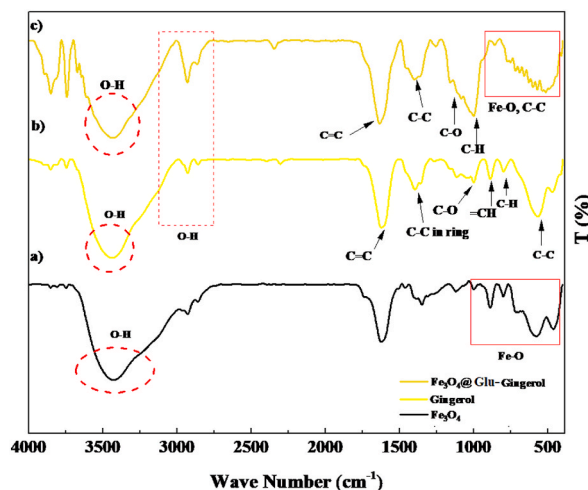
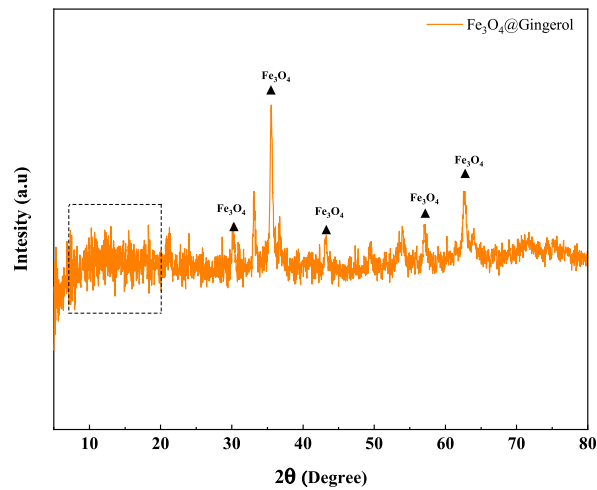

Fig. 1. FT-IR analysis of Fe_3O_4@Glu-Gingerol NPs.
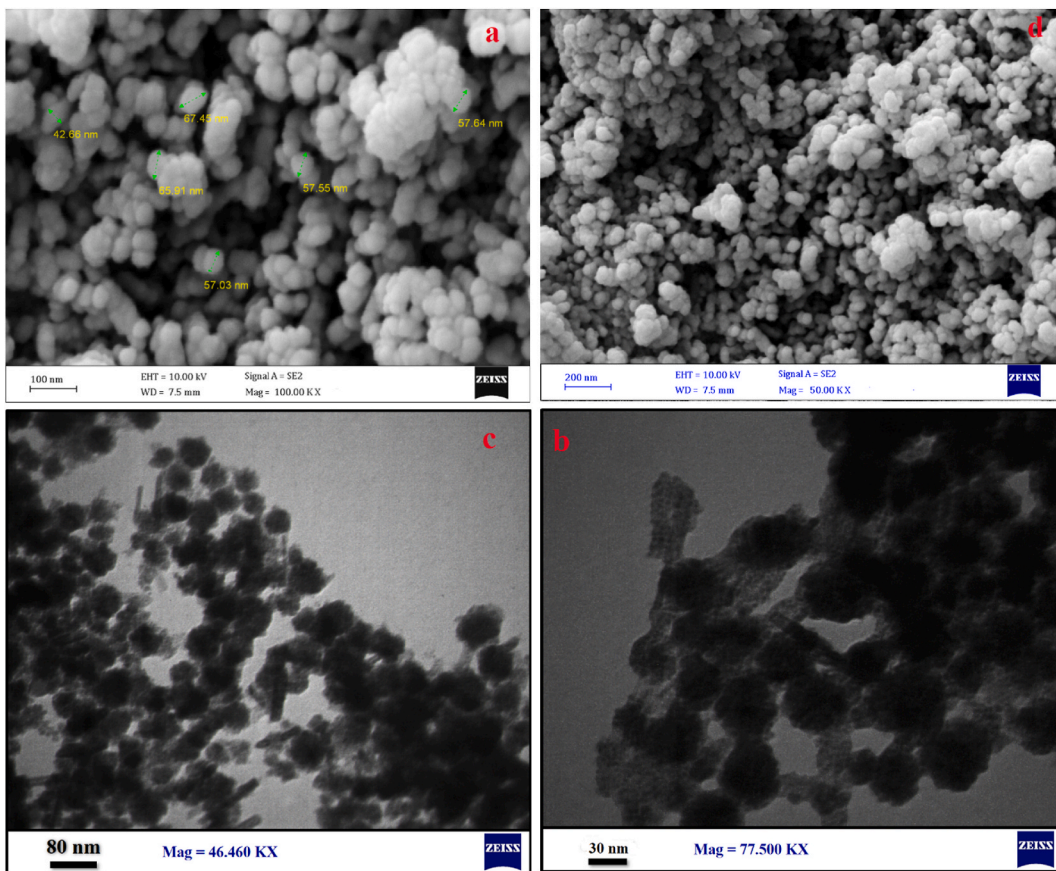
Fig. 2. XRD pattern of Fe$_3$O$_4$@Glu-Gingerol NPs.

Fig. 3. SEM (a, d), and TEM (b, c) images of Fe$_3$O$_4$@Glu-Gingerol NPs.

3.4. Expression of apoptosis signaling genes

Studying the effect of Fe$_3$O$_4$@Glu-Gingerol on the expression of the *CASP8*, *BAX*, and *BCL2* genes showed that treatment of the Fe$_3$O$_4$@Glu-Gingerol significantly up-regulated the *BAX* and *CASP8* genes, and attenuated the *BCL2* gene. According to the results, the *BAX* and *CASP8* were upregulated by 2.8 and 2.49 folds, respectively. In contrast, the *BCL2* gene was attenuated by 0.75 folds. Meanwhile, the relative expression of the *BAX* and *CASP8* in Fe$_3$O$_4$ treated cells was up-regulated by 1.4 and 1.38 folds, respectively. In
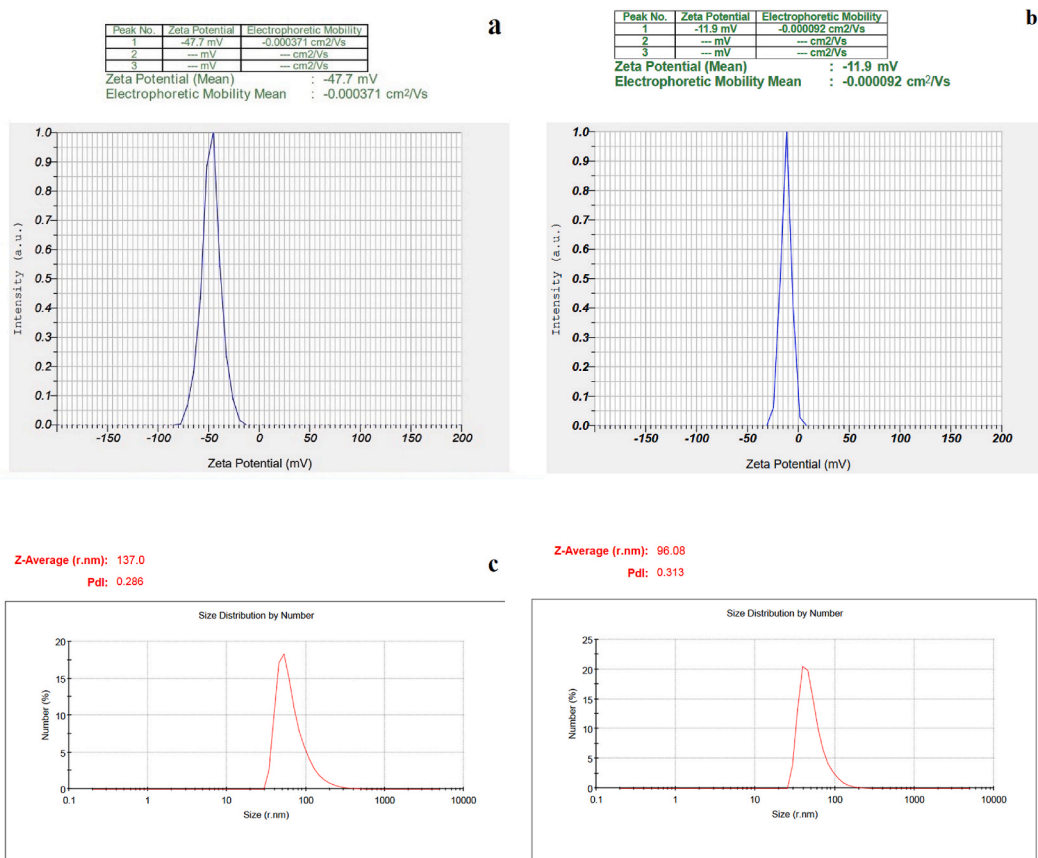
Fig. 4. Surface charge and DLS analyses of Fe$_3$O$_4$@Glu-Gingerol and Fe$_3$O$_4$ NPs. (a): Zeta potential of Fe$_3$O$_4$@Glu-Gingerol, (b): Zeta potential of Fe$_3$O$_4$ NP, (c): DLS analysis of Fe$_3$O$_4$@Glu-Gingerol and (d): DLS analysis of Fe$_3$O$_4$ NP.

contrast, the *BCL2* gene in Fe$_3$O$_4$ NPs treatment group had a reduced expression by 0.91 folds (Fig. 9).

3.5. Caspase 3 activity and hoechst staining

We observed that the Fe$_3$O$_4$@Glu-Gingerol increased the activity of the caspase 3 by 2.8 folds (Fig. 10a) and Fe$_3$O$_4$ NPs increased the activity by 1.38 folds (Fig. 10b). According to the Hoechst staining, treating lung adenocarcinoma cells with Fe$_3$O$_4$@Glu-Gingerol caused morphological nuclear alterations associated with cell apoptosis, including chromatin fragmentation, the presence of apoptotic bodies, and chromatin condensation (Fig. 11a and b).

4. discussion

The frequency of Lung cancer associated mortality has been increasing which indicates the inefficiency of current diagnosis and therapeutic approaches. After the emergence of nanotechnology, many researchers seek novel nanotechnology products for cancer diagnosis and treatment. For this purpose, the development of supermagnetic NPs for site-directed delivery of drugs has been considered. Owing to the good biocompatibility, minor side effects, and supermagnetic feature, the use of Fe$_3$O$_4$ in biomedicine has gained considerable interest. Therefore, we aimed to design Fe$_3$O$_4$ NPs functionalized with glucose and conjugated with gingerol, as a therapeutic component.

Characterization of the synthesized nanoparticles suggests that gingerol was properly conjugated with Fe$_3$O$_4$ NPs after functionalization with glucose. The nanoparticles were synthesized at the nanoscale and had spherical morphology which may improve their biological activities by increasing the efficiency of their penetration into the cell. Moreover, regarding their magnetic properties, the nanoparticles can be employed for targeted therapy using an external magnetic field. Furthermore, the negative surface charge of the particles provides sufficient repulsive force between the particles to reduce particle agglomeration, which is an essential characteristic required for their biomedical applications.

In addition to the supermagnetic property, the cytotoxic potential of Fe$_3$O$_4$ NPs for several cancer cells has been reported. The anticancer activity of Fe$_3$O$_4$ NPs contributes to the generation of reactive oxygen species (ROS). Due to the strong oxidation potential,
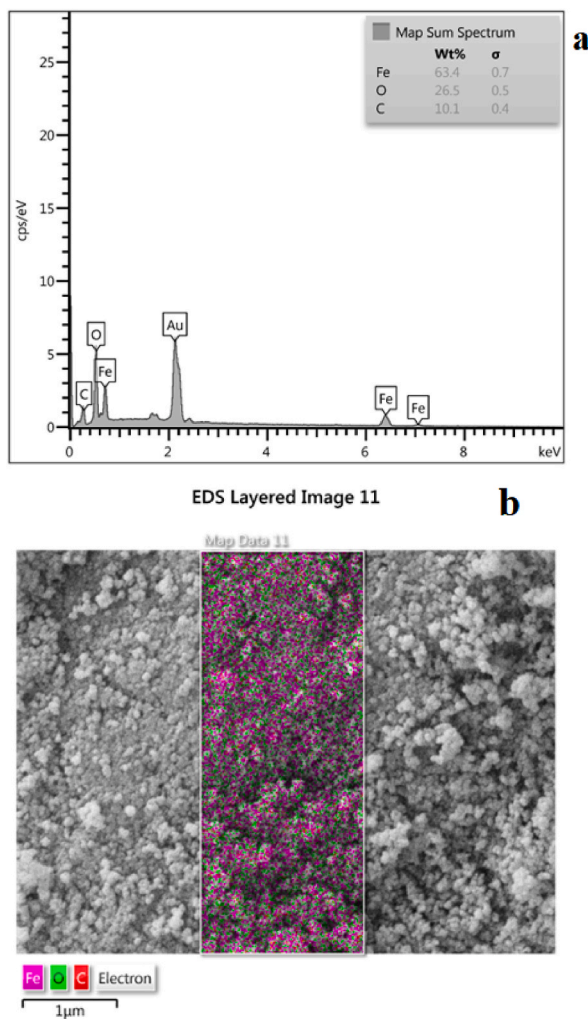
Fig. 5. EDS (a) and mapping (b) of Fe_3O_4@Glu-Gingerol NPs.

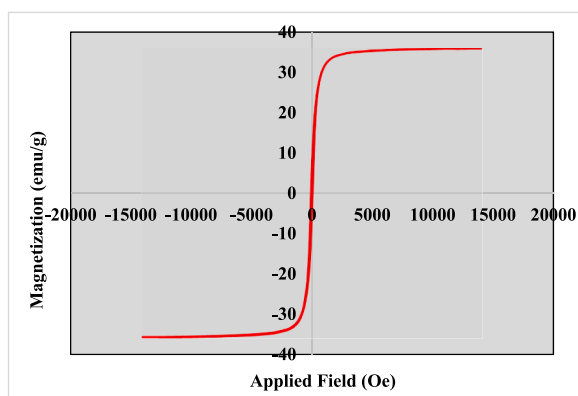**Fig. 6.** Magnetic saturation curve of Fe_3O_4@Glu-Gingerol NPs.

the generation of ROS can damage cell structures leading to protein oxidative carbonylation, lipid peroxidation, nucleic acid breakage, and destruction of membrane structure [18,19]. Moreover, the ROS molecule could damage the cell membrane which in turn, could increase the penetration of the drugs into the cancer cell.
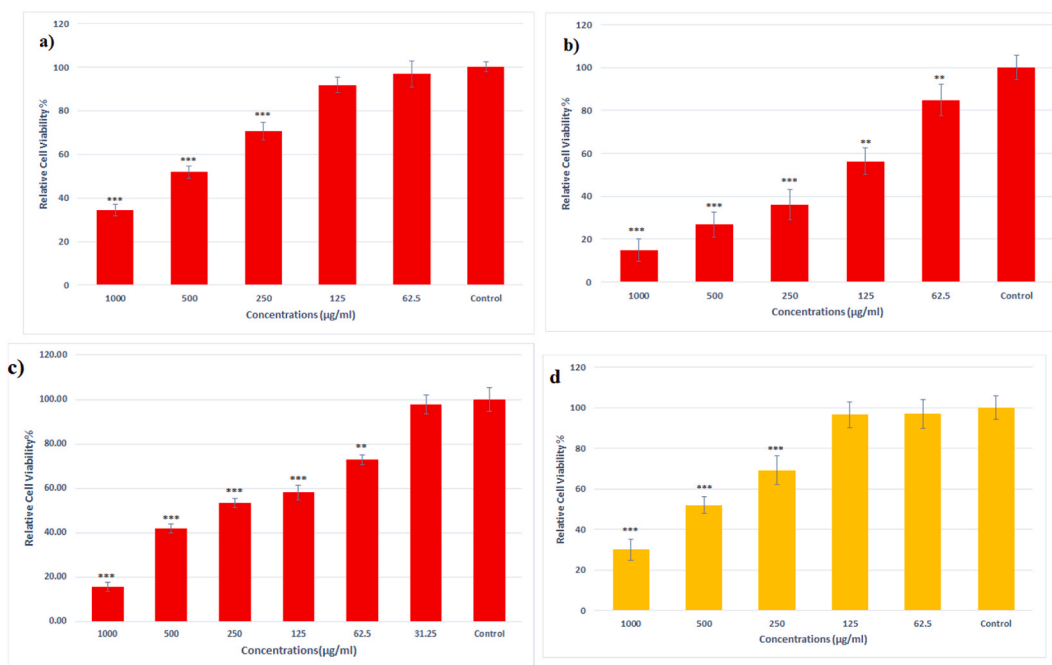
Fig. 7. Cytotoxicity of Fe_3O_4@Glu-Gingerol on a) MRC-5 cell line, b) A549 cell line, c) Gingerol on A549 cancer cell line and d) Fe_3O_4 NPs on A549 cancer cell line. Data are stated as mean ± SD. Asterisks (*) show a significant difference with control group (*** = $P < 0.001$, ** = $P < 0.01$, * = $P < 0.05$).
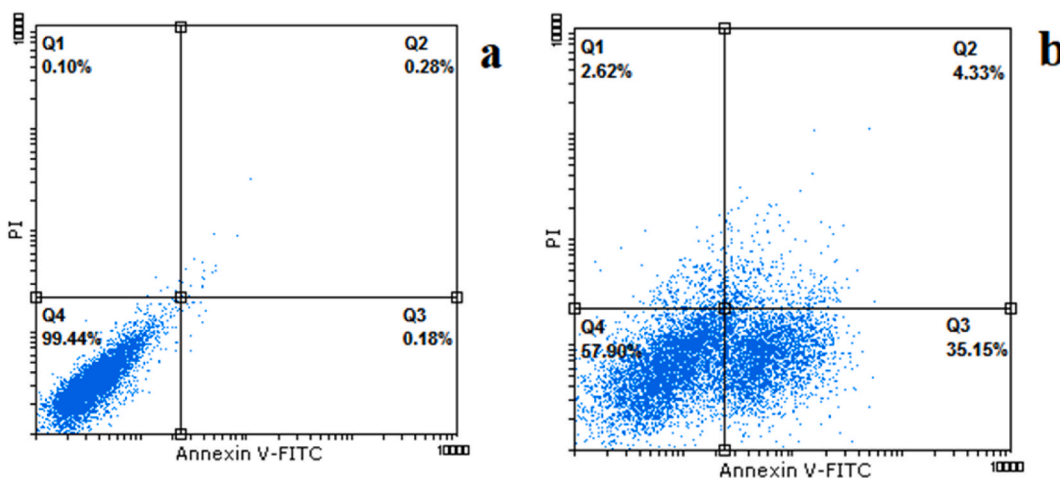

Fig. 8. Flow cytometry analysis of a) control, and b) treated cells.

Several studies reported the anticancer activity of gingerol for several cancer cells [20]. It was found that gingerol is able to bind nuclear DNA, avoiding the operation of the enzymes responsible for DNA replication and transcription, which may in turn cause cell cycle arrest and apoptosis induction [20]. In addition, it was found that gingerol could arrest the cell cycle and induce apoptosis through the activation of Caspase 3, 7, 8, and 9 [21]. Several studies showed that the activity of caspase-8 increases during apoptosis. Drug-induced activation of caspase-8 may occur through the both death receptor and mitochondrial pathways. Caspase-8 can be triggered after activation of caspase-9, and through the activity of caspases-3 and -6 [22].

Comparison of the cytotoxic activity of Fe_3O_4@Glu-Gingerol for lung adenocarcinoma and healthy human cells we found that the prepared NPs had a considerably greater toxic effects on cancer cells than normal cell line. The higher susceptibility of cancer cells may be related to their high metabolic rate and nutrient demand which increase their membrane permeability to the extracellular compounds. Glucose is considered the most preferred and major carbon source for human cells, and cancer cells naturally have higher glucose intake and consumption than normal cells [23]. The synthesized NPs contain glucose molecules which may facilitate their

Fig. 9. The effect of Fe₃O₄@Glu-Gingerol and Fe₃O₄ NPs on expression of *CASP8, BCL2*, and *BAX* genes in lung adenocarcinoma cells. Data are stated as mean ± SD. Asterisks (*) show a significant difference with control group (*** = $P < 0.001$, ** = $P < 0.01$, * = $P < 0.05$).
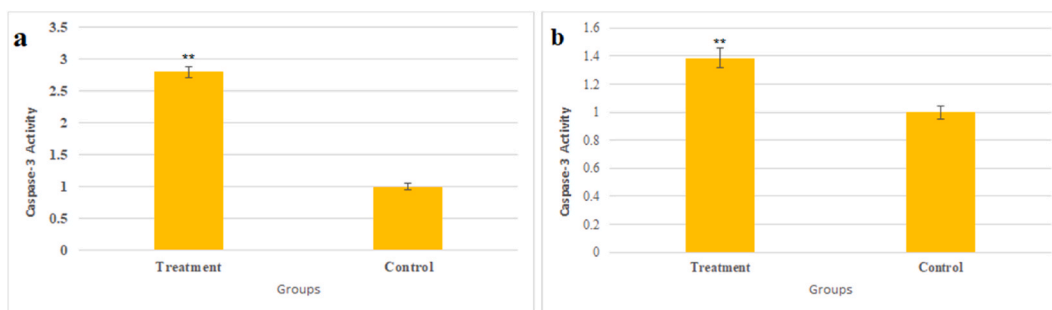
Fig. 10. The effect of (a) Fe₃O₄@Glu-Gingerol and (b) Fe₃O₄ NPs on activity of Caspase 3 protein in control and treated cells. Data are stated as mean ± SD. Asterisks (*) specify a significant difference in comparison to control group (*** = $P < 0.001$, ** = $P < 0.01$, * = $P < 0.05$).

internalization into the cancer cells which may result in a higher susceptibility of lung cancer cells than MRC-5 cells. Compared with gingerol, Fe₃O₄@Glu-Gingerol NPs had a stronger anti-cancer effect on lung cancer cells that indicates the effect of Iron oxide nanoparticles on improving the effectiveness of gingerol, which can probably be explained by strengthening the penetration rate of
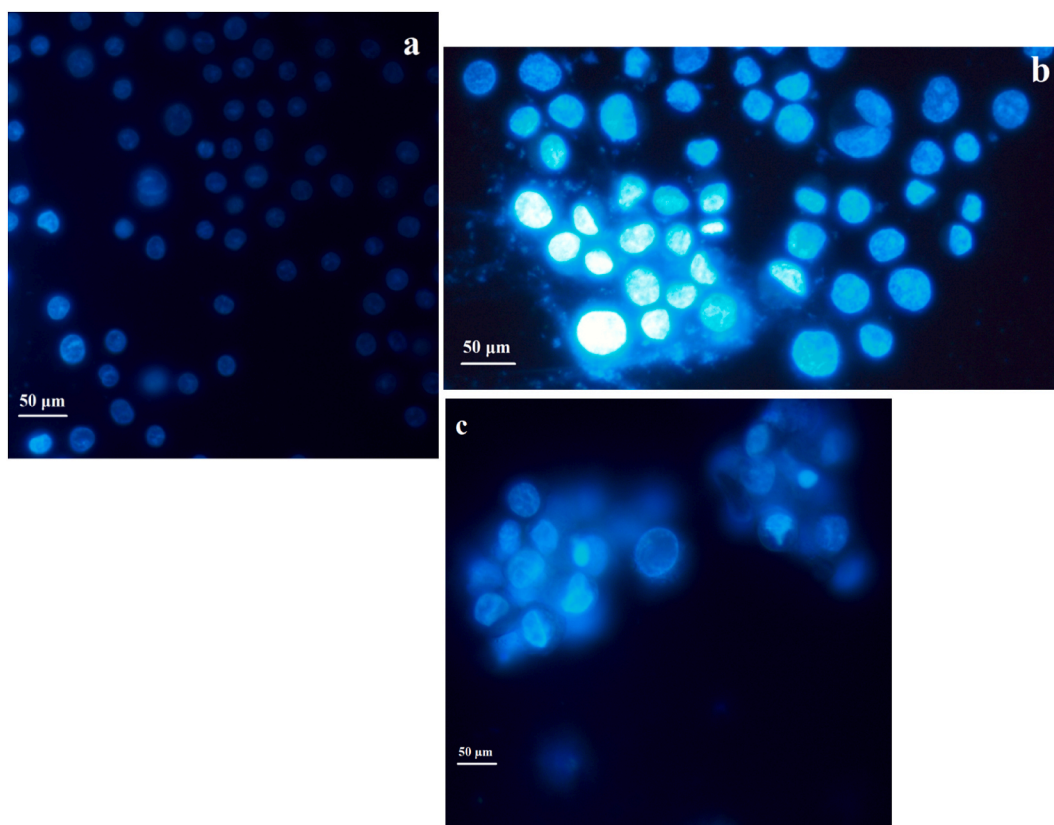
Fig. 11. The Hoechst staining of control cells (a), and the cells treated with Fe$_3$O$_4$@Glu-Gingerol (b) and Fe$_3$O$_4$ NPs (c).

gingerol into the cell by Iron oxide nanoparticles.

Flow cytometry analysis showed that treatment with the nanoparticles can significantly increase cell apoptotic. In other words, it seems that treating with Fe$_3$O$_4$@Glu-Gingerol triggered apoptotic pathways in lung cancer cells. Cell apoptosis occurs through two main pathways, including the extrinsic or cytoplasmic pathway and the intrinsic or mitochondrial pathway. The extrinsic pathway is triggered through the Fas death receptor, which activates the initiator caspases −8 and −10. In contrast, the intrinsic pathway causes cytochrome-c release from the mitochondrial membrane and activating the initiator caspase-9. Both pathways lead to the activation of the caspase cascade resulting in the cleavage of regulatory and structural molecules and cell death [24].

Based on this study, Fe$_3$O$_4$@Glu-Gingerol remarkably promoted the expression of the proapoptotic genes, *CASP8* and *BAX*. As described above, caspase 8 is an initiator caspase that contributes to the activation of extrinsic apoptosis pathways in response to extracellular stimuli. Therefore, the upregulation of the *CASP8* gene suggests the activation of extrinsic apoptosis in Fe$_3$O$_4$@Glu-Gingerol cells. Furthermore, there is a close association between these two apoptotic pathways so that the protein Bid, which is activated by caspase 8 can be transferred to the mitochondria leading to the release of cytochrome *c* from the mitochondrial membrane through the activity of the proapoptotic proteins such as the BAX and BAK, while the anti-apoptotic proteins such as the Bcl-2, are usually inhibited. Therefore, triggering the extrinsic apoptosis leads to the initiation of the intrinsic pathway as well [25].

The BAX is a pro-apoptotic protein that is involved in activating of the intrinsic apoptosis through the increase of mitochondrial outer membrane permeabilization, while BCL2 is a BAX inhibitor protein [26]. As was observed in this work, treating lung adenocarcinoma cells with Fe$_3$O$_4$@Glu-Gingerol led to upregulation of the *CASP8* and *BAX* genes, while it down-regulated the *BCL2* gene. Therefore, it can be concluded that treating lung adenocarcinoma cells with Fe$_3$O$_4$@Glu-Gingerol can activate of the extrinsic apoptosis pathway and subsequently triggers the intrinsic pathway as well.

Caspases are a group of proteases that play a crucial role in the programmed cell death. Activated caspase 8 can interact with cell death receptors and initiates extrinsic apoptotic signaling pathways [27]. The activity of Caspase-3 in nanoparticle treatment group considerably increased which is in agreement with the upregulation of the *BAX* and *CASP8* genes that suggests the activation of intrinsic and extrinsic apoptosis by Fe$_3$O$_4$@Glu-Gingerol.

A significantly increased activity of Caspase 3 was also noticed in nanoparticle treatment group, suggesting the activation of caspase-dependent apoptosis initiation. Previous studies showed that gingerol could induce autophagy and caspase 3-dependent apoptosis, which is in agreement with our results [21]. Moreover, the Hoechst staining revealed the apoptosis associated alterations in treated cells that are in agreement with other findings.

5. Conclusions

This study showed that Fe_3O_4@Glu-Gingerol has considerable antiproliferative effects on lung adenocarcinoma cell line through activating the intrinsic and extrinsic apoptosis pathways. Due to the considerable anticancer potential of gingerol and supermagnetic properties of iron oxide nanoparticles, Fe_3O_4@Glu-Gingerol is a promising anticancer agent that can be further evaluated at in-vivo experiments to be used in lung cancer treatment.

Ethics approval and consent to participate

Not applicable.

Consent for publication

The authors give the publisher the permission to publish this work.

Data availability statement

Data will be made available on request.

CRediT authorship contribution statement

Tabarek Abdulrazaq Alkinani: Resources, Methodology, Formal analysis, Conceptualization. **Fahimeh Abedini Bajgiran:** Writing - original draft, Resources. **Mohammad Rezaei:** Resources. **Ali Motamedi Maivan:** Resources, Investigation, Formal analysis. **Fatemeh Jafari Golrokh:** Resources. **Mona Bejarbaneh:** Writing - original draft, Resources. **Sara Rezaei Mojdehi:** Writing - original draft, Resources. **Sahar Gorji:** Writing - original draft, Resources. **Reza Ghasemian:** Resources. **Mohammad Dashtban Jalil Pustin Sarai:** Writing - original draft, Resources. **Fatemeh Akbari:** Writing - original draft, Resources. **Somayeh Dehghan:** Writing - original draft, Resources. **Fatemeh Mirzaee:** Resources, Investigation, Formal analysis. **Noor Hussein Abdulrahman:** Resources. **Ali Salehzadeh:** Writing - review & editing, Supervision, Methodology, Investigation, Formal analysis, Conceptualization.

Declaration of Competing interest

The authors declare that they have no known competing financial interests or personal relationships that could have appeared to influence the work reported in this paper.

References

[1] H. Sung, J. Ferlay, R.L. Siegel, M. Laversanne, I. Soerjomataram, A. Jemal, F. Bray, Global cancer statistics 2020: GLOBOCAN estimates of incidence and mortality worldwide for 36 cancers in 185 countries, CA A Cancer J. Clin. 71 (3) (2021) 209–249, https://doi.org/10.3322/caac.21660.
[2] R. Awasthi, A. Roseblade, P.M. Hansbro, M.J. Rathbone, K. Dua, M. Bebawy, Nanoparticles in cancer treatment: opportunities and obstacles, Curr. Drug Targets 19 (14) (2018) 1696–1709, https://doi.org/10.2174/1389450119666180326122831.
[3] B.L. Lin, X.D. Shen, S. Cui, Application of nanosized Fe_3O_4 in anticancer drug carriers with target-orientation and sustained-release properties, Biomed. Mater. 2 (2) (2007) 132, https://doi.org/10.1088/1748-6041/2/2/011.
[4] Y. Liu, Z. Chen, J. Wang, Systematic evaluation of biocompatibility of magnetic Fe 3 O 4 nanoparticles with six different mammalian cell lines, J. Nanoparticle Res. 13 (2011) 199–212, https://doi.org/10.1007/s11051-010-0019-y.
[5] D.C. Kennedy, G. Orts-Gil, C.H. Lai, L. Müller, A. Haase, A. Luch, P.H. Seeberger, Carbohydrate functionalization of silver nanoparticles modulates cytotoxicity and cellular uptake, J. Nanobiotechnol. 12 (1) (2014) 1–8, https://doi.org/10.1186/s12951-014-0059-z.
[6] M. Morais, V. Machado, F. Dias, P. Figueiredo, C. Palmeira, G. Martins, R. Fernandes, A.R. Malheiro, K.S. Mikkonen, A.L. Teixeira, R. Medeiros, Glucose-functionalized silver nanoparticles as a potential new therapy agent targeting hormone-resistant prostate cancer cells, Int. J. Nanomed. (2022) 4321–4337, https://doi.org/10.2147/IJN.S364862.
[7] Y.A. Mohd Yusof, Gingerol and its role in chronic diseases, Drug discovery from mother nature (2016) 177–207, https://doi.org/10.1007/978-3-319-41342-6_8.
[8] A.A. Oyagbemi, A.B. Saba, O.I. Azeez, Molecular targets of [6]-gingerol: its potential roles in cancer chemoprevention, Biofactors 36 (3) (2010) 169–178, https://doi.org/10.1002/biof.78.

[9] S.H. Lee, M. Cekanova, S.J. Baek, Multiple mechanisms are involved in 6-gingerol-induced cell growth arrest and apoptosis in human colorectal cancer cells, Mol. Carcinog.: Published in cooperation with the University of Texas MD Anderson Cancer Center 47 (3) (2008) 197–208, https://doi.org/10.1002/mc.20374.

[10] M. Su, X. Wang, G. Cao, L. Sun, R.J. Ho, Y. Han, Y. Hong, D. Wu, Prediction of the potential mechanism of compound gingerol against liver cancer based on network pharmacology and experimental verification, J. Pharm. Pharmacol. 74 (6) (2022) 869–886, https://doi.org/10.1093/jpp/rgac002.

[11] E.K. Radhakrishnan, S.V. Bava, S.S. Narayanan, L.R. Nath, A.K.T. Thulasidasan, E.V. Soniya, R.J. Anto, [6]-Gingerol induces caspase-dependent apoptosis and prevents PMA-induced proliferation in colon cancer cells by inhibiting MAPK/AP-1 signaling, PLoS One 9 (8) (2014), e104401, https://doi.org/10.1371/journal.pone.0104401.

[12] R. Nasiri, N. Arsalani, Y. Panahian, One-pot synthesis of novel magnetic three-dimensional graphene/chitosan/nickel ferrite nanocomposite for lead ions removal from aqueous solution: RSM modelling design, J. Clean. Prod. 201 (2018) 507–515, https://doi.org/10.1016/j.jclepro.2018.08.059.

[13] M. Hosseinkhah, R. Ghasemian, F. Shokrollahi, S.R. Mojdehi, M.J.S. Noveiri, M. Hedayati, M. Rezaei, A. Salehzadeh, Cytotoxic potential of nickel oxide nanoparticles functionalized with glutamic acid and conjugated with thiosemicarbazide (NiO@ Glu/TSC) against human gastric cancer cells, J. Cluster Sci. 33 (5) (2022) 2045–2053, https://doi.org/10.1007/s10876-021-02124-2.

[14] R. Kumari, A.K. Saini, A. Kumar, R.V. Saini, Apoptosis induction in lung and prostate cancer cells through silver nanoparticles synthesized from Pinus roxburghii bioactive fraction, JBIC, J. Biol. Inorg. Chem. 25 (2020) 23–37, https://doi.org/10.1007/s00775-019-01729-3.

[15] M.W. Pfaffl, A new mathematical model for relative quantification in real-time RT–PCR, Nucleic Acids Res. 29 (9) (2001), https://doi.org/10.1093/nar/29.9.e45 e45-e45.

[16] Y. Xu, L. Liu, X. Qiu, Z. Liu, H. Li, Z. Li, W. Luo, E. Wang, CCL21/CCR7 prevents apoptosis via the ERK pathway in human non-small cell lung cancer cells, PLoS One 7 (3) (2012), e33262, https://doi.org/10.1371/journal.pone.0033262.

[17] A.P. Sharif, K. Habibi, Z.K. Bijarpas, H.F. Tolami, T.A. Alkinani, M. Jameh, A.A. Dehkaei, S.K. Monhaser, H.B. Daemi, A. Mahmoudi, R.S. Masouleh, Cytotoxic effect of a novel GaFe$_2$O$_4$@ Ag nanocomposite synthesized by scenedesmus obliquus on gastric cancer cell line and evaluation of BAX, bcl-2 and CASP8 genes expression, J. Cluster Sci. 34 (2) (2023) 1065–1075, https://doi.org/10.1007/s10876-022-02288-5.

[18] M.F. Zaltariov, M. Hammerstad, H.J. Arabshahi, K. Jovanovic, K.W. Richter, M. Cazacu, S. Shova, M. Balan, N.H. Andersen, S. Radulović, J. Reynisson, New iminodiacetate–thiosemicarbazone hybrids and their copper (II) complexes are potential ribonucleotide reductase R2 inhibitors with high antiproliferative activity, Inorg. Chem. 56 (6) (2017) 3532–3549. https://pubs.acs.org/doi/abs/10.1021/acs.inorgchem.6b03178.

[19] S. Swathi, F. Ameen, G. Ravi, R. Yuvakkumar, S.I. Hong, D. Velauthapillai, M.D. AlKahtani, M. Thambidurai, C. Dang, Cancer targeting potential of bioinspired chain like magnetite (Fe3O4) nanostructures, Curr. Appl. Phys. 20 (8) (2020) 982–987, https://doi.org/10.1016/j.cap.2020.06.013.

[20] Z. Yu, Q. Li, J. Wang, Y. Yu, Y. Wang, Q. Zhou, P. Li, Reactive oxygen species-related nanoparticle toxicity in the biomedical field, Nanoscale Res. Lett. 15 (1) (2020) 1–14, https://doi.org/10.1186/s11671-020-03344-7.

[21] D. Chakraborty, K. Bishayee, S. Ghosh, R. Biswas, S.K. Mandal, A.R. Khuda-Bukhsh, [6]-Gingerol induces caspase 3 dependent apoptosis and autophagy in cancer cells: drug–DNA interaction and expression of certain signal genes in HeLa cells, Eur. J. Pharmacol. 694 (1–3) (2012) 20–29, https://doi.org/10.1016/j.ejphar.2012.08.001.

[22] C.B. Lin, C.C. Lin, G.J. Tsay, 6-Gingerol inhibits growth of colon cancer cell LoVo via induction of G2/M arrest, Evid. base Compl. Alternative Med. (2012), https://doi.org/10.1155/2012/326096, 2012.

[23] J. Liu, H. Uematsu, N. Tsuchida, M.A. Ikeda, Essential role of caspase-8 in p53/p73-dependent apoptosis induced by etoposide in head and neck carcinoma cells, Mol. Cancer 10 (1) (2011) 1–13, https://doi.org/10.1186/1476-4598-10-95.

[24] K. Birsoy, R. Possemato, F.K. Lorbeer, E.C. Bayraktar, P. Thiru, B. Yucel, T. Wang, W.W. Chen, C.B. Clish, D.M. Sabatini, Metabolic determinants of cancer cell sensitivity to glucose limitation and biguanides, Nature 508 (7494) (2014) 108–112, https://doi.org/10.1038/nature13110.

[25] I.M. Ghobrial, T.E. Witzig, A.A. Adjei, Targeting apoptosis pathways in cancer therapy, CA A Cancer J. Clin. 55 (3) (2005) 178–194, https://doi.org/10.3322/canjclin.55.3.178.

[26] M. Brentnall, L. Rodriguez-Menocal, R.L. De Guevara, E. Cepero, L.H. Boise, Caspase-9, caspase-3 and caspase-7 have distinct roles during intrinsic apoptosis, BMC Cell Biol. 14 (2013) 1–9, https://doi.org/10.1186/1471-2121-14-32.

[27] B. Tummers, D.R. Green, Caspase-8: regulating life and death, Immunol. Rev. 277 (1) (2017) 76–89, https://doi.org/10.1111/imr.12541.